ASKAP Commissioning Update #8

November 2015

Welcome to the eighth edition of the ASKAP Commissioning Update. This includes latest results from commissioning activities with the six-antenna 'Boolardy Engineering Test Array' (BETA), an overview of the Memo Series associated with these activities and some details on the work underway with the Mk II ASKAP PAFs. We hope you enjoy receiving this regular update on the progress of ASKAP commissioning. Don't hesitate to contact us if you have any questions.

Ant Schinckel	***Lisa Harvey-Smith***	***Dave McConnell***
ASKAP Project Director	*ASKAP Project Scientist*	*ASKAP Commissioning and Early Science Manager*

This edition of the ASKAP Commissioning Updates resumes the series after a 15-month gap. Its purpose is to inform members of the ASKAP community about the recent advances in technical understanding of ASKAPs operation and performance. In this issue, because of the gap in the series of Updates, we summarise all the Technical Memoranda that have been prepared since commissioning began. In future updates we will report any new Memos.

Construction and Commissioning Status

Murchison Radio-astronomy Observatory (MRO): Construction of the permanent observatory power station has commenced; it is a hybrid plant that will use both diesel generators, photovoltaic solar cells and a large lithium battery storage system.

Boolardy Engineering Test Array (BETA): the 6-antenna array (Antennas 1, 3, 6, 8, 9, and 15) equipped with Mk I PAFs. For the past few months, BETA has been reduced to five antennas since the cooling failed in the PAF on Antenna 9.

Recent usage of BETA has been:

- Experimental beamforming, aiming to constrain the position and shape of beams more closely than is possible with the standard "Maximum-Signal-to-Noise" algorithm.
- T_{sys} and efficiency measurements using drift scans of the Galactic Plane.
- Testing of the procedures being developed for calibration of antenna pointing.
- Early RFI mitigation experiments.
- Continued search for red-shifted HI by the FLASH team.

ASKAP

- Four antennas now equipped with Mk II PAFs – ASKAP Antennas 2, 4, 5, 12
- Two PAFs are at the MRO awaiting mounting on Antennas 13, 14.

- The prototype Mk II PAF is mounted on Antenna 29 and is being used to test the prototype On-Dish-Calibration (ODC) system.
- Verification and commissioning of the first four Mk II antenna/PAF systems has begun. Aidan Hotan and Max Voronkov report steady progress over several commissioning sessions at the MRO over the past three months. In general the configuration and operation of the Mk II systems, and associated firmware and software, is easier to manage than was BETA at this stage in its development.
- A brief report of early Mk II images and performance estimates is available on page 7 of this Update.

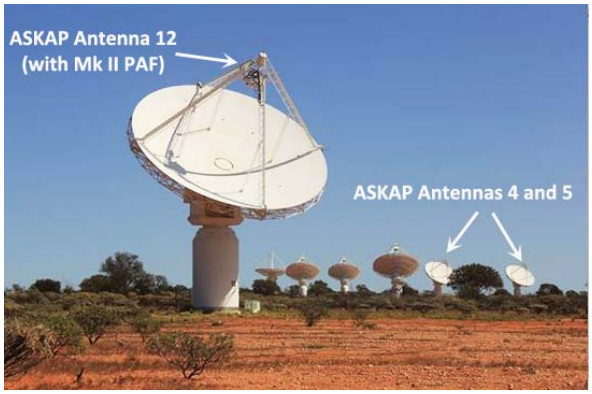

The three ASKAP antennas installed with Mk II PAFs to produce the newest images.

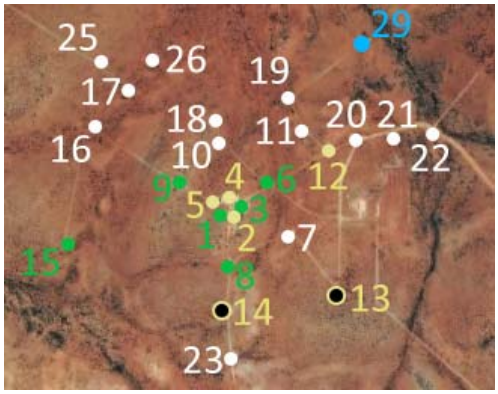

A close-up of the ASKAP antenna core, highlighting those with Mk I PAFs (in green) and MkII PAFs (in yellow), as well as Antenna 29 (in blue, installed with the Mk II prototype).

Technical memoranda

ASKAP Commissioning and Early Science (ACES) Technical memos are posted on the ATNF website at: http://www.atnf.csiro.au/projects/askap/ACES-memos.

Below we give summaries of each.

001 Beam geometry in ASKAP by J.E.Reynolds

The geometry of the AKSAP Phased Array Feeds is described. Coordinate systems in the focal plane, both rectilinear and polar, are defined with reference to the axis of the primary reflector, to the tetrapod support legs, and to the zero point of the antenna's roll axis.

The numbering scheme used for the 188 PAF elements is defined and the location of all elements in the defined coordinate frames given. The relationship between the focal plan and sky coordinates is given, in particular how the position of an off-axis image on the PAF relates to the astronomically-defined Position Angle on the sky.

The memo applies the concept of "plate scale" to the PAF and its geometrical relationship with sky coordinates. (The plate scale is simply related to what radio engineers refer to as a "beam deviation factor".)

Finally, and importantly, the memo deals with the formation of beams, how their position in the sky relates to the position of their PAF elements in the focal plane, and the most convenient coordinate frames for defining arrangements (footprints) of multiple beams.

002 Initial characterisation of BETA polarimetric response by R.J.Sault

Results are presented of initial polarimetric tests with the Boolardy Engineering Test Array (BETA) and its Mk I PAFs.

The memo begins by introducing the polarimetric properties of the ASKAP PAFs and antennas, including orientations of linear sensors, how that determines the calculation of Stokes U and Q, and the parallactifying action of the ASKAP antenna roll axis. BETA has no injected noise system, and so X-Y phase was estimated by intentionally rotating one antenna 5 degrees about its roll axis.

Two calibration sources, B1934-638 and 3C138, were observed in the 700 – 1000 MHz band with axial X and Y beams formed using the standard MaxSNR method. Observations were made twice with a six-week interval between, and with the calibration sources at beam centre.

Leakages derived from the B1934-638 observations were indistinguishable from zero (apart from the effects of zero-point calibration errors on the antennas' roll axes) and stable over the six weeks.

B1934-638 was also observed with a 42 arcmin offset from beam centre; the same low level of leakages was evident. 3C138 has pronounced and well characterised polarisation; global ionospheric models were used to correct the measured polarization position angle, and the results were in agreement with the expected values.

The memo points out the importance of knowledge of the shapes of the X and Y beams for successful wide-field polarimetry.

003 The ASKAP Roll Axis—Preliminary study of its benefits to calibration and imaging by I.Heywood et al

A standard test field containing numerous strong sources has been observed twice with the ASKAP BETA system, with the third axis of motion – the roll axis – disabled for the second run.

These two data sets are subjected to identical calibration and imaging pipelines in order to gauge the effects of the roll axis when observing with a Phased Array Feed.

Present beam forming techniques only allow meaningful comparisons to be performed with the on axis 'boresight' beam. Observing with the roll axis tracking reduces the standard deviation of the close-in imaging artefacts around the bright sources by factors of 2–3.

Applying directional calibration techniques and examining the solutions reveals that the elevated artefacts are imparted by position and time dependent gain drifts with amplitude modulations of up to 50%, consistent with a rotating primary beam of non-trivial shape.

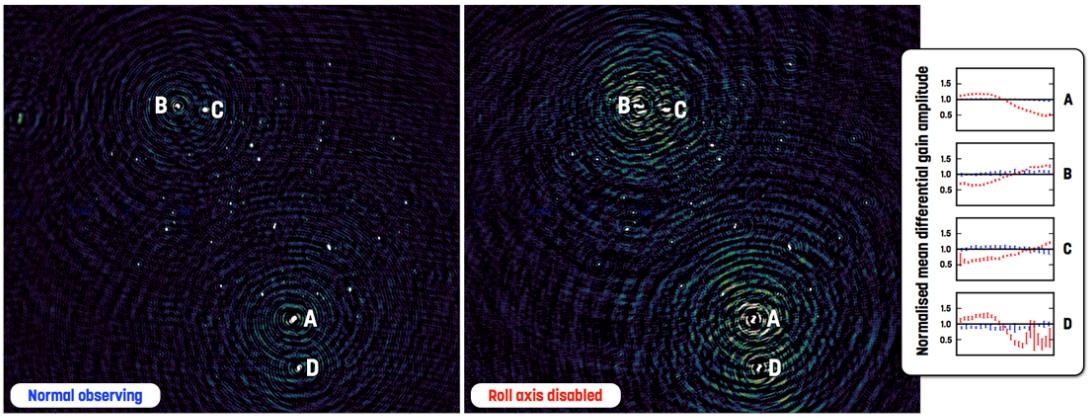

> An observation performed with the roll axis engaged (left) shows a clear improvement in image quality compared to an otherwise identical observation with the roll axis disabled (right). Both data sets were subjected to an identical calibration and imaging pipeline. The inset panel shows the differential gain amplitudes associated with the four dominant sources in the field. The red points correspond to the observation with the roll axis disabled, and demonstrate the level to which the roll axis (blue points) suppresses time and position dependent gain drifts. Credit: CSIRO.

004 Delay calibration of the Phased Array Feed using observations of the South Celestial Pole by K.Bannister & A.Hotan

The Boolardy Engineering Test Array (BETA) forms beams digitally by the weighted sum of up to 188 phased array feed (PAF) elements.

Initially, we expected that the relative complex gains of the elements should only drift slowly with time, necessitating infrequent updates to the beam weights. During commissioning observations we noticed that beam sensitivity and quality would decay on time scales of days to weeks, with weights more likely to suffer catastrophic degradation after a major power cycle of the BETA equipment. This degradation has been traced to step changes in delay between individual elements. These are due to the random start-up phase of a clock divider in the digitisers.

The current setup and calibration software associated with this hardware module does not adequately compensate for the fact that the digitisers can start in one of several clock states. This should be fixable in the long term.

Here we describe a method for measuring the inter-element delays by observing the South celestial pole, and show that the corrections made using the astronomical delay compensation machinery remove the inter-element delays.

005 ASKAP antenna aperture efficiency estimation by D. McConnell et al

We describe a procedure for estimating system noise and aperture efficiency for elements of a radio synthesis array. The method uses the known flux-density of a cosmic calibration source and knowledge of the variation in sky brightness to scale the visibility noise and determine the antenna sensitivity—the increment of antenna temperature for a given increment of incident power flux-density.

We apply this to the six ASKAP antennas currently equipped with Mk I Phased Array Feeds (PAFs) at a frequency of 1390MHz for which we have a reliable model of the sky brightness temperature. The results are summarised in the following table.

Antenna	K (mk/Jy)	Efficiency	T_{sys} (K)
AK01	25.5	0.67	110.3
AK03	27.3	0.67	98.6
AK06	27.8	0.68	109.4
AK08	29.0	0.71	112.6
AK09	31.1	0.76	117.8
AK15	29.8	0.73	117.4

Table: Results summary of the analysis for the axial beam on all BETA antennas.

006 The outer six antennas and the WALLABY and EMU survey times for a 30 PAF ASKAP array by I. Heywood

Working on the assumption that ASKAP will consist of 30 antennas equipped with Mk II PAFs, some discussion is now underway as to which of the 36 antennas should form the array.

The effects of visibility weighting must be taken into account in order to perform an assessment of a configuration as EMU is wholly dependent on this being efficient.

I present a method for assessing the effects of weighting for any given configuration, the outputs of which are an estimation of the increase in survey time for EMU and WALLABY over that of the ASKAP-36 case.

007 Widefield polarimetric considerations for ASKAP by R.J.Sault

This builds on the earlier memo on BETA polarimetric characterisation (here-after Memo#2). It considers issues with widefield polarimetric observations with the current BETA system, and makes suggestions for implementing wide- field polarimetric processing on ASKAP.

The conclusions are:

- The ASKAP antennas and BETA hardware have good and stable polari- metric response. The different BETA antennas show the same response, which will simplify the processing needed for widefield polarimetric imaging.
- The ability of BETA (and ultimately the full ASKAP) to produce quality widefield polarimetric images is critically dependent on the algorithm used to determine the beamformer weights. The algorithm currently used for BETA is inadequate. More broadly, the beamforming algorithm will affect the mosaicing capability of ASKAP. There is a need to develop better algorithms to determine the beamformer weights.
- Correction for both widefield instrumental polarization and ionospheric Faraday rotation can probably be achieved without the need for so-called A-projection algorithms.

008 Optimisation of the 2-km core of ASKAP–30 by T. Westmeier (UWA)

This document describes three different core configurations for ASKAP-30 that were investigated with respect to their performance for WALLABY.

All configurations assume that the outer antennas (32, 33, 34, and 36) are included, while Antennas 31 and 35 are left out. Hence, the problem reduces to removing four antennas from the 30-antenna core of ASKAP.

The three configurations tested include:

1. The **default** ASKAP-30 configuration put forward by CASS and submitted to AAL:
    - This configuration has the four outermost available antennas within the 2-km core that are not part of either BETA or ASKAP-12, removed.
    - Such a configuration essentially results in the most compact possible core and hence provides maximum sensitivity at lower resolution (≈ 30”), making it suitable for WALLABY and GASKAP.
2. An **optimised** configuration (“Optimised”) with the most Gaussian UV coverage in the core.
    - This configuration was created by fitting a Gaussian to the radial UV histogram of the 2-km core of all possible ASKAP-30 configurations and then selecting the one that results in the best fit with the lowest RMS.
    - Again, all ASKAP-12 antennas were required to be included, but BETA antennas were not.
    - This configuration results in a slightly more extended core than the “CASS” configuration by removing some of the inner antennas (including Antenna 1), but its UV coverage is more homogeneous, resulting in lower sidelobe levels and better sensitivity at higher resolution (≈ 20”–25”), making it suitable for DINGO and FLASH.
3. A **compromise** configuration (“Compromise”) that was created in a similar way as “Optimised”, but this time also requiring BETA Antennas 1 and 3 to be included to ensure that all of the shortest baselines are present.
    - This configuration is meant to be a compromise between point-source sensitivity and surface brightness sensitivity.

Configurations Working Group Final Recommendation for ASKAP-30

Our brief: The currently funded 30 ASKAP antennas equipped with Mk II PAFs is significantly different to the 36 originally proposed so there is a need to decide on a 30 element configuration that balances the impact on the key SSPs (EMU And WALLABY) while maximizing the science that can be delivered.

CSIRO established a small working group with representation from both key projects to address the various issues, identify the key criteria and recommend a baseline 30-antenna configuration to present to all the SST's, and to the broader community, for comment.

In summary, the recommended ASKAP-30 configuration is all antennas except 7, 11, 21, 29, 31, and 35 (option 2 in memo#008, above). For more information, see the ASKAP Science Case Memo Series (028): http://www.atnf.csiro.au/projects/askap/askap-science-case-memos

First ASKAP images using Mk II Phased Array Feeds

M. Voronkov, A. Hotan, J. Reynolds, D. McConnell

2015 October 29

We report the first radio images from ASKAP using its second generation (Mk II) Phased Array Feeds (PAFs). These images result from early commissioning trials of four antennas, their PAFs and the associated digital spectrometers, beamformers and correlator.

Two images have been made, one of source B0407-658 and the other of the Apus field.

The Apus Image has 16 formed (synthetic) beams, more than any other radio image to date. The details of the two images are listed below.

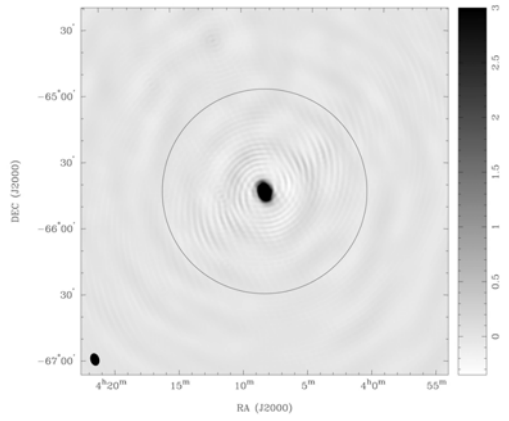

Field	B0407-658
Centre frequency	939.5 MHz
Bandwidth	48 MHz
Antennas	AK02, AK04, AK05, AK12
Beams	Single boresight beam formed using "MaxSNR" method from observations of the Sun.
Bandpass calibration	B1934-638
Integration time	9.44h
Image peak	13 Jy
Image noise	6mJy (Thermal noise estimate 0.9mJy)

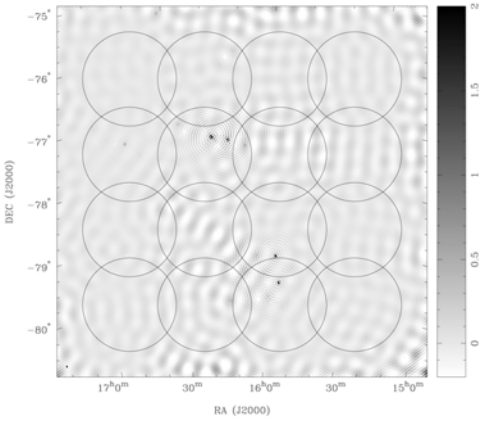

Field	Apus (16-beam linear mosaic)
Centre frequency	939.5 MHz
Bandwidth	48 MHz
Antennas	AK04, AK05, AK12
Beams	16 in a 4x4 footprint, formed using "MaxSNR" method from observations of the Sun.
Bandpass calibration	1934-638, but problems with absolute flux calibration
Integration time	12.08h
Image peak	~6 Jy
Image noise	~10mJy

Both images reported were made from a single linear polarization. The data were processed (calibration and imaging) in ASKAPsoft. Note that the ASKAP antennas do not yet have any reference noise source for gain calibration and stabilization.

This, and the small number of antennas available, leads to the image noise being significantly higher than the expected thermal noise.

Associated with each image, all beams were calibrated using an observation of B1934-638. We have used these observations to estimate the system noise over the observing band (48MHz, centred at 939.5 MHz).

Our estimate, averaged over all 16 Beams is $T_{sys}/\eta \approx 111 \pm 19$ K.

We note that this estimate, for which we used the cross-hand polarization product XY, suffers from a lack of polarimetric calibration and therefore could be an overestimate.

The comparatively high uncertainty in the figure (19K) reflects some systematic effects that we are yet to understand, but could relate to the polarimetric calibration or to our inexperience in beamforming with the Mk II PAFs.

Our Estimate for T_{sys}/η is within 1- σ of the aperture-array measurement previously reported for the prototype Mk II PAF. Together, these images demonstrate a working telescope with the performance of most major sub-systems proven.

In particular, these results are the first demonstration of the Mk II PAFs In an interferometer.

Telescope integration, verification and commissioning will continue to refine the assessments of performance.